The Eurasia Proceedings of Science, Technology, Engineering & Mathematics (EPSTEM)
ISSN: 2602-3199

The Eurasia Proceedings of Science, Technology, Engineering and Mathematics (EPSTEM), 2025

Volume 33, Pages 130-139

IConTech 2025: International Conference on Technology

Influence of Different Behavior in Tension and Compression on Longitudinal Fracture of Inhomogeneous Beams Under Impact

Victor Rizov
University of Architecture, Civil Engineering and Geodesy

Abstract: The current paper has for its purpose to develop a theoretical investigation of the effect of different mechanical behavior in tension and compression on the longitudinal fracture in continuously inhomogeneous beam structures subjected to impact loading. The basic motive for carrying-out this investigation is the fact that in many situations in engineering practice various beam structures are under impact loading which may be induced, for instance, by falling objects which strike the structure. This kind of loading threatens the structural integrity and reliable functioning of engineering constructions. Therefore, it is important to study in detail different aspects of the behavior of structures under impact. This paper is focused on the influence of different mechanical behavior in tension and compression on the longitudinal fracture. The beams under consideration are non-linear elastic and exhibit continuous inhomogeneity along their thickness. The integral *J* is applied for studying the longitudinal fracture under impact loading. The strain energy release rate is obtained to verify the solution of the integral *J*. Results illustrating the effect of different behavior in tension and compression are derived and presented in graphical form.

Keywords: Impact loading, Longitudinal fracture, Inhomogeneous beam structure

Introduction

The quick development of continuously inhomogeneous (functionally graded) structural materials has a significant influence on the state of various branches of modern engineering (Kaul, 2014; Toudehdehghan et al., 2017; Gandra et al., 2011). The strong interest which the representatives of the international engineering community around the globe show towards the continuously inhomogeneous materials is conditioned mainly by their excellent properties (Mahamood & Akinlabi, 2017). Among them, one of the most important advantages of these new engineering materials in comparison with the traditional homogeneous materials like metals or heterogeneous (fiber reinforced) composites is the continuous variation of their properties along one or more directions in a given structural member (Radhika et al., 2020; Riov, 2018). Besides, the variation of the material properties can be tailored during manufacturing in order to achieve some predefined goals (Gururaja Udupa et al., 2014; Fanani et al., 2021). However, the increasing application of these highly efficient materials requires elaboration and practical use of different methods for analyzing the behavior and performance of structural members and components subjected to various external influences. In the context of safety, studying fracture behavior of continuously inhomogeneous structural members under different loading conditions is of primary importance (Dowling, 2007; Rizov, 2019, 2024).

The current paper focuses on analyzing the effects of different mechanical behavior in tension and compression on longitudinal fracture in continuously inhomogeneous load-bearing beam structures under impact loading. The beams under consideration have non-linear elastic behavior. The material exhibits continuous inhomogeneity along the beam thickness. The beam hosts a longitudinal crack. The impact loading is induced by a falling object that strikes the beam. The longitudinal fracture behavior of the beam under impact is analyzed by applying the integral *J*.

The strain energy release rate (SERR) under impact loading is derived for verification of the integral J solution. A parametric study is carried out by applying the solution. The results of the parametric study are reported in the form of graphs. The study provides a useful knowledge for the influence of different mechanical behavior in tension and compression on longitudinal fracture of continuously inhomogeneous non-linear elastic engineering structures subjected to impact loading.

Theoretical Investigation

The load-bearing beam structure depicted in Figure 1 is subjected to impact loading by a small object of weight, P, which falls from height, h_P, and strikes the upper surface of the beam in point, B_4.

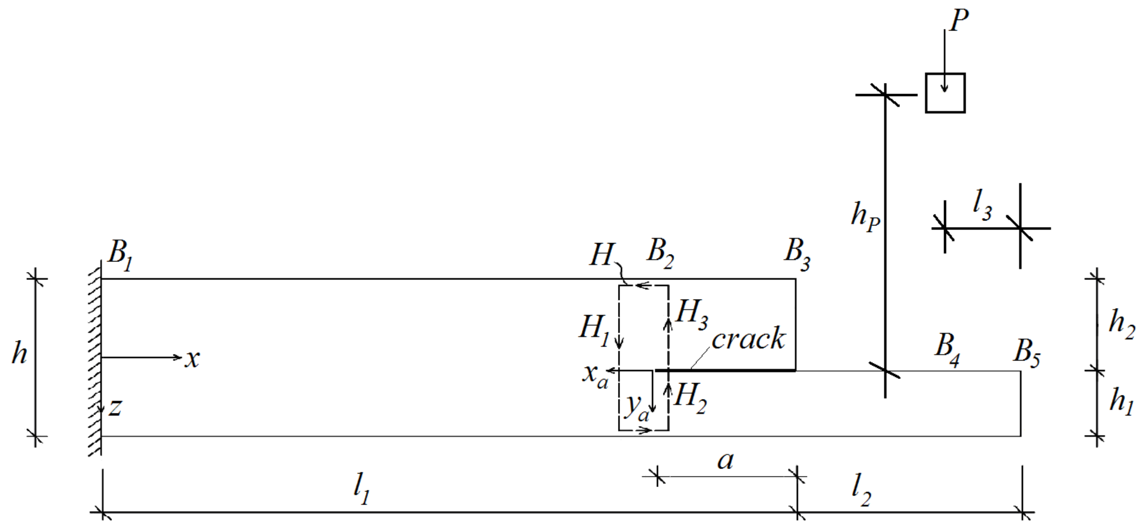

Figure 1. Inhomogeneous beam structure under impact loading

The beam is clamped in its left-hand end. The right-hand end of the beam is free. The thickness of the beam in portion, B_1B_3, is h. In section, B_3, the beam thickness changes abruptly. In portion, B_3B_5, the thickness is h_1. The beam hosts a longitudinal crack of length, a, in portion, B_2B_3.

The material of the beam has non-linear elastic behavior that obeys the Ramberg-Osgood law (Dowling, 2007). In compression, the behavior is described by the stress-strain relation presented in Eq. (1).

$$\varepsilon_c = \frac{\sigma_c}{E_c} + \left(\frac{\sigma_c}{D_c}\right)^{\frac{1}{n_c}}, \tag{1}$$

where ε_c is the strain, σ_c is the stress, E_c, D_c and n_c are material parameters. The stress-strain relation in tension is presented in Eq. (2).

$$\varepsilon_t = \frac{\sigma_t}{E_t} + \left(\frac{\sigma_t}{D_t}\right)^{\frac{1}{n_t}}. \tag{2}$$

Here, ε_t is the strain, σ_t is the stress, E_t, D_t and n_t are material parameters in tension.

The material of the beam is continuously inhomogeneous along the thickness. The change of material parameters across the beam thickness is given below.

$$E_c = E_{cup} + \frac{E_{clw} - E_{cup}}{h^{\alpha}}\left(\frac{h}{2} + z\right)^{\alpha}, \tag{3}$$

$$D_c = D_{cup} + \frac{D_{clw} - D_{cup}}{h^{\beta}}\left(\frac{h}{2} + z\right)^{\beta}, \tag{4}$$

$$n_c = n_{cup} + \frac{n_{clw} - n_{cup}}{h^{\eta}}\left(\frac{h}{2} + z\right)^{\eta}, \tag{5}$$

$$E_t = E_{tup} + \frac{E_{tlw} - E_{tup}}{h^{\lambda}}\left(\frac{h}{2} + z\right)^{\lambda}, \tag{6}$$

$$D_t = D_{tup} + \frac{D_{tlw} - D_{tup}}{h^{\rho}}\left(\frac{h}{2} + z\right)^{\rho}, \tag{7}$$

$$n_t = n_{tup} + \frac{n_{tlw} - n_{tup}}{h^{\omega}}\left(\frac{h}{2} + z\right)^{\omega} \tag{8}$$

where

$$-\frac{h}{2} \leq z \leq \frac{h}{2} \tag{9}$$

Here E_{cup}, D_{cup} and n_{cup} are the values of E_c, D_c and n_c on the upper surface of the beam, E_{clw}, D_{clw} and n_{clw} are the values of E_c, D_c and n_c on the lower surface of the beam. Analogically, E_{tup}, D_{tup} and n_{tup} are the values of E_t, D_t and n_t on the upper surface of the beam, while E_{tlw}, D_{tlw} and n_{tlw} are the values of properties in tension on the lower surface of the beam. The parameters, α, β, η, λ, ρ and ω, govern the change of E_c, D_c, n_c, E_t, D_t and n_t, respectively.

The longitudinal fracture under impact is analyzed theoretically by using the integral *J* (Broek, 1986). The integration is performed long the contour *H* that is shown in Figure 1. Since the contour *H* has three portions, H_1, H_2 and H_3, the solution of *J* is obtained as

$$J = J_{H1} + J_{H2} + J_{H3}. \tag{10}$$

The solution of *J* in portion, H_1, is given in Eq. (11).

$$J_{H1} = J_{H1c} + J_{H1t}, \tag{11}$$

where J_{H1c} and J_{H1t} are the solutions in the compression and tension zones, respectively. J_{H1c} and J_{H1t} are presented below, i.e.

$$J_{H1c} = \int\left[u_{0c}\cos\alpha_c - \left(p_{xac}\frac{\partial u}{\partial x_a} + p_{yac}\frac{\partial v}{\partial x_a}\right)\right]ds, \tag{12}$$

$$J_{H1t} = \int \left[u_{0t} \cos\alpha_t - \left(p_{xat} \frac{\partial u}{\partial x_a} + p_{yat} \frac{\partial v}{\partial x_a} \right) \right] ds \tag{13}$$

The components of J_{H1c} are found as

$$u_{0c} = \int \sigma_c d\varepsilon \,, \tag{14}$$

$$\cos\alpha_c = 1 \,, \tag{15}$$

$$p_{xac} = -\sigma_c \,, \tag{16}$$

$$\frac{\partial u}{\partial x_a} = \varepsilon \,, \tag{17}$$

$$p_{yac} = 0 \,, \tag{18}$$

$$ds = dz_1 \,, \tag{19}$$

where σ_c is the stress in the compression zone, ε is the strain, α_c is the inclination of the integration contour, u is the axial displacement, u is the transversal displacement, z_1 is the vertical centric axis of the beam cross-section.

The quantities involved in Eq. (13) are determined as written below

$$u_{0t} = \int \sigma_t d\varepsilon \,, \tag{20}$$

$$\cos\alpha_t = 1 \,, \tag{21}$$

$$p_{xat} = \sigma_t \,, \tag{22}$$

$$\frac{\partial u}{\partial x_a} = \varepsilon \,, \tag{23}$$

$$p_{yat} = 0 \,, \tag{24}$$

$$ds = dz_1 \,, \tag{25}$$

where σ_t is the stress in the tension zone.

The stresses are found by using the dynamic coefficient, k_{dyn}, i.e.

$$\sigma_c = k_{dyn} \sigma_{cst} \,, \tag{26}$$

$$\sigma_t = k_{dyn} \sigma_{tst} \,, \tag{27}$$

where σ_{cst} and σ_{tst} are the stresses in compression and tension induced by the static force of magnitude, P, applied in point, B_4, on the upper surface of the beam. The dynamic coefficient is determined by applying the approach reported in (Obodovski & Hanin, 1981). This approach leads to Eq. (28) for k_{dyn}.

$$k_{dyn} = 1 + \sqrt{1 + 2\frac{h_P}{\delta_{st}}\frac{P}{P + G_{bm}}} \quad , \tag{28}$$

where δ_{st} is the static displacement of point, B_4. G_{bm} is the deadweight of the beam structure.

The static displacement is found by using the integrals of Maxwell-Mohr, i.e.

$$\delta_{st} = \sum \int \kappa_i M_i dx \, , \tag{29}$$

where κ_i is the curvature, M_i is the bending moment induced by a unit vertical force applied in point, B_4.

In order to derive the curvatures, we first analyze the distribution of the strains along the thickness of the beam in portion, B_1B_2, by applying Eq. (30).

$$\varepsilon = \kappa_i (z_1 - z_{1n}), \tag{30}$$

Where

$$-\frac{h}{2} \leq z_1 \leq \frac{h}{2} \, . \tag{31}$$

Here, z_{1n} is the neutral axis coordinate.

Then, the curvature and the neutral axis coordinate are determined by using Eqs. (32) and (33).

$$N = \iint_{(A_c)} \sigma_c dA + \iint_{(A_t)} \sigma_t dA \, , \tag{32}$$

$$M = \iint_{(A_c)} \sigma_c z_1 dA + \iint_{(A_t)} \sigma_t z_1 dA \, , \tag{33}$$

where N is axial force, M is the bending moment, A_c and A_t are the areas of compression and tension zones of the beam cross-section, respectively. N and M are found as

$$N = 0 \, , \tag{34}$$

$$M = P(l_1 + l_2 - l_3 - x), \tag{35}$$

where the distances, l_1, l_2 and l_3, are defined in Figure 1. The MatLab is used for solving Eqs. (32) and (33).

The solution of the *J* integral in portion, H_2, of the integration contour is derived by performing replacements in Eqs. (11) – (25).

The upper crack arm is free of stresses. Therefore, we have

$$J_{H3} = 0 \tag{36}$$

Finally, the *J* integral solution is found by using Eq. (10). The integration is performed by the MatLab.

The SERR, G, is derived to verify the *J* integral solution. For this purpose, the expression reported in (Rizov, 2018) is applied, i.e.

$$G = \frac{1}{b}\left(\iint_{(A_{H2c})} u^{*}_{0H2c} dA + \iint_{(A_{H2t})} u^{*}_{0H2t} dA - \iint_{(A_{H1c})} u^{*}_{0c} dA - \iint_{(A_{H1t})} u^{*}_{0t} \right), \tag{37}$$

where A_{H2c} and A_{H2t} are the compression and tension zones in the cross-section of the lower crack arm behind the crack tip, A_{H1c} and A_{H1t} are the compression and tension zones in the cross-section of the beam ahead of the crack tip, u^{*}_{0H2c} and u^{*}_{0H2t} are the complementary strain energy densities in compression and tension in the lower crack arm behind the crack tip, u^{*}_{0H1c} and u^{*}_{0H1t} are the complementary strain energy densities in compression and tension in the beam ahead of the crack tip. The complementary strain energy densities in compression and tension in the beam ahead of the crack tip are obtained by Eqs. (38) and (39), respectively.

$$u^{*}_{0H1c} = \sigma_c \varepsilon - u_{0c}, \tag{38}$$

$$u^{*}_{0H1t} = \sigma_t \varepsilon - u_{0t}, \tag{39}$$

where u_{0c} and u_{0t} are determined by Eq. (14) and Eq. (20), respectively. The complementary strain energy densities in compression and tension in the lower crack arm behind the crack tip are found by performing replacements in Eqs. (38) and (39). The SERR found by using Eq. (37) matches the solution of the integral *J* derived by Eq. (10) which is a verification of the solution.

Parametric Study

The parametric study reported in this section of the paper aims to evaluate how the longitudinal fracture of the inhomogeneous beam under impact loading is affected by the different mechanical behavior in tension and compression.

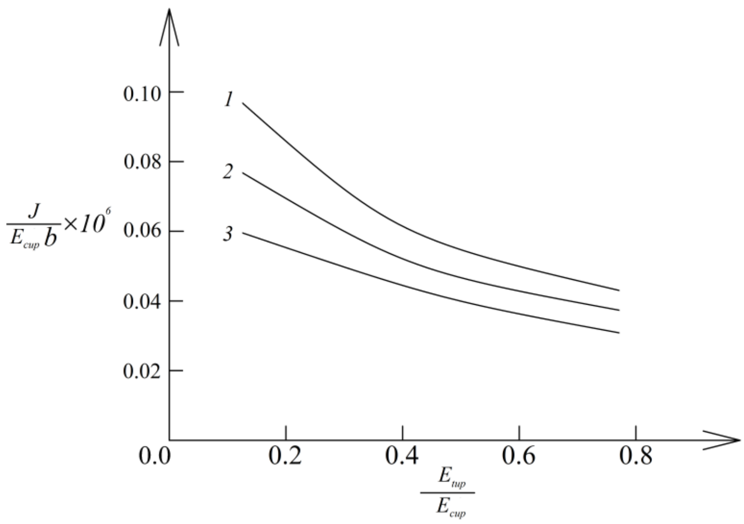

Figure 2. The integral *J* plotted versus E_{tup} / E_{cup} ratio

The effects of material inhomogeneity and the impact loading parameters are evaluated too. It is assumed that $b = 0.015$ m, $h = 0.020$ m, $l_1 = 0.300$ m, $l_2 = 0.300$ m, $l_3 = 0.050$ m, $a = 0.150$ m, $\alpha = 0.4$, $\beta = 0.4$, $\eta = 0.4$, $\lambda = 0.6$, $\rho = 0.6$ and $\omega = 0.6$. The parametric study yields the results shown in graphical form in Figures 2, 3, 4, 5 and 6.

Figure 2 illustrates how the integral *J* in normalized form changes when E_{tup} / E_{cup} ratio varies at $l_3 / l_1 = 1/6$ (curve 1), $l_3 / l_1 = 2/6$ (curve 2) and $l_3 / l_1 = 3/6$ (curve 3). The ratio, l_3 / l_1, determines the location of the impact loading application point on the beam surface.

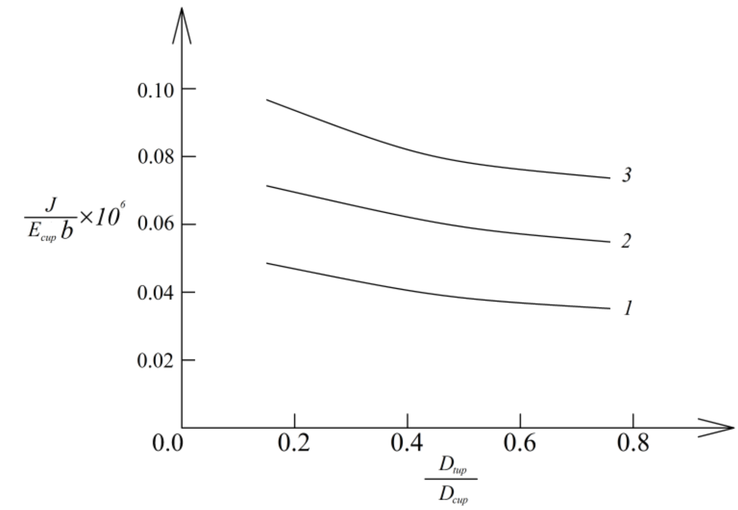

Figure 3. The integral *J* plotted versus D_{tup} / D_{cup} ratio

It can be seen in Figure 2 that the value of the integral *J* reduces as a result of increase of l_3 / l_1 ratio (this is due to decrease of the bending moment in the beam). Increase of E_{tup} / E_{cup} ratio leads also to reduction of the integral *J* (Figure 2).

One can observe the effect of D_{tup} / D_{cup} ratio on the value of the integral *J* at $h_P / l_2 = 0.3$ (curve 1), $h_P / l_2 = 0.6$ (curve 2) and $h_P / l_2 = 0.9$ (curve 3) in Figure 3.

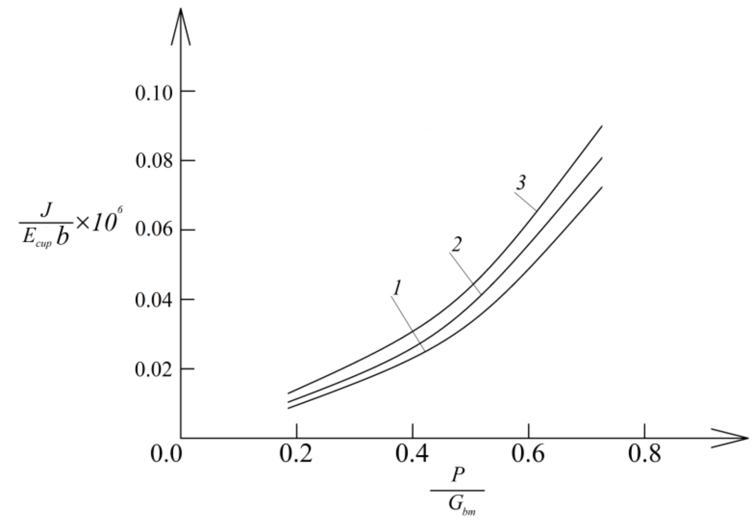

Figure 4. The integral *J* plotted versus P / G_{bm} ratio

The graphs indicate that the integral *J* decreases when D_{tup} / D_{cup} ratio grows. However, grow of h_P / l_2 ratio induces a significant rise of the value of the integral *J* (Figure 3). This observation is attributed to increase of the impact energy. The graphs reported in Figure 4 illustrate how the integral *J* is affected by the change of P / G_{bm} ratio at $n_{tup} / n_{cup} = 0.2$ (curve 1), $n_{tup} / n_{cup} = 0.5$ (curve 2) and $n_{tup} / n_{cup} = 0.8$ (curve 3).

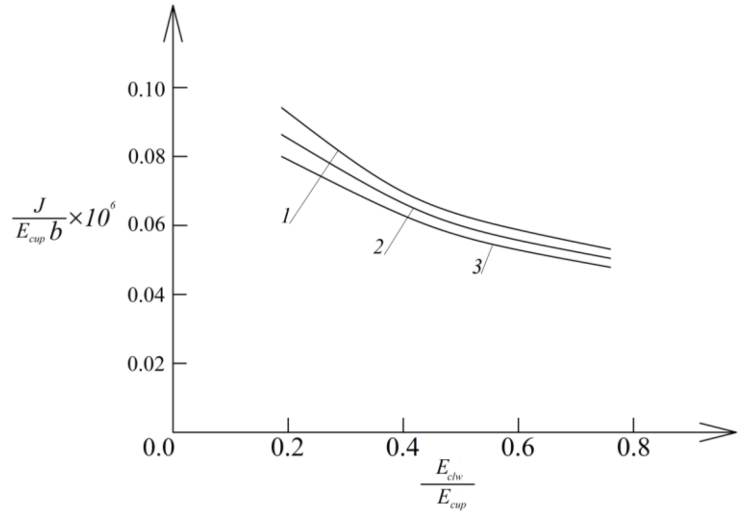

Figure 5. The integral *J* plotted versus E_{clw} / E_{cup} ratio

It can be seen in Figure 4 that the integral *J* increases its value when n_{tup} / n_{cup} ratio grows. Increase of the integral *J* value is observed also at increase of P / G_{bm} ratio (this behavior is due to rise of the impact energy).

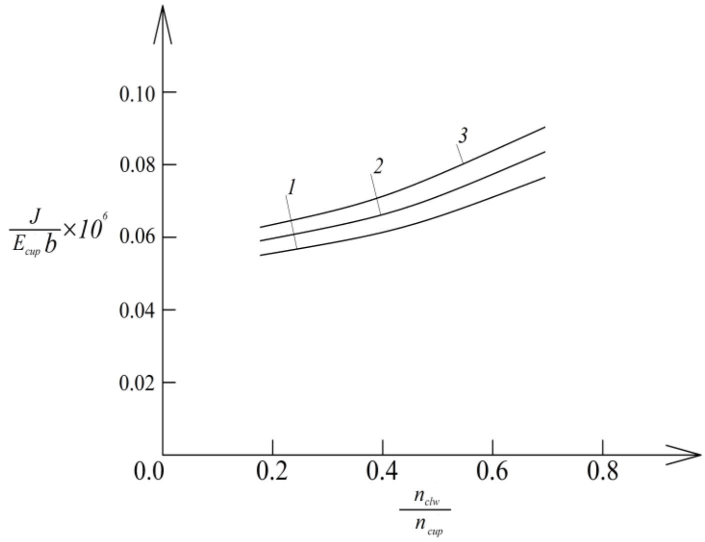

Figure 6. The integral *J* plotted versus n_{clw} / n_{cup} ratio

One can get an idea for the variation of the value of the integral *J* due to continuous material inhomogeneity from the graphs shown in Figures 5 and 6. The inhomogeneity is characterized by the E_{clw} / E_{cup}, D_{clw} / D_{cup}, n_{clw} / n_{cup} and n_{tlw} / n_{tup} ratios. The graphs in Figure 5 illustrate the effect of E_{clw} / E_{cup} ratio at $D_{clw} / D_{cup} = 0.2$ (curve 1), $D_{clw} / D_{cup} = 0.5$ (curve 2) and $D_{clw} / D_{cup} = 0.8$ (curve 3). Figure 6 shows the effect of n_{clw} / n_{cup} ratio at $n_{tlw} / n_{tup} = 0.3$ (curve 1), $n_{tlw} / n_{tup} = 0.5$ (curve 2) and $n_{tlw} / n_{tup} = 0.8$ (curve 3). The graphs in Figure 5 indicate a reduction of the value of the integral *J* when the

E_{clw} / E_{cup} and D_{clw} / D_{cup} ratios grow. Increase of n_{clw} / n_{cup} and n_{tlw} / n_{tup} ratios generate growth of the *J* integral value as can be seen in Figure 6.

Conclusion

The effect of different mechanical behavior in tension and compression on the longitudinal fracture of continuously inhomogeneous beam structures subjected to impact loading is investigated theoretically. Solution of the integral *J* is obtained. The SERR under impact loading is derived for verification of the solution. A parametric study is performed by using the solution. The study indicates that the longitudinal fracture is affected significantly by the different behavior in tension and compression. For example, it is observed that the value of the integral *J* reduces when E_{tup} / E_{cup} and D_{tup} / D_{cup} ratios grow. The growth of n_{tup} / n_{cup} ratio generates rise of the *J* integral. It is found that the integral *J* value decreases when l_3 / l_1 ratio grows. An increase of the value of the integral *J* is detected when h_P / l_2 ratio rises. The study of the effect of material inhomogeneity reveals reduction of the integral *J* when E_{clw} / E_{cup} and D_{clw} / D_{cup} ratios grow. The rise of n_{clw} / n_{cup} and n_{tlw} / n_{tup} ratios, however, leads to growth of the integral *J* value.

Recommendations

The theoretical investigation developed in this paper can be used in structural design of continuously inhomogeneous inhomogeneous beams with different mechanical behavior in tension and compression under impact loading.

Scientific Ethics Declaration

* The author declares that the scientific ethical and legal responsibility of this article published in EPSTEM Journal belongs to the author.

Conflict of Interest

* The author declares that he has no conflicts of interest.

Funding

*This study received no external funding.

Acknowledgements or Notes

* This article was presented as an oral presentation at the International Conference on Technology (www.icontechno.net) held in Trabzon/Türkiye on May 01-04, 2025.

References

Broek, D. (1986). *Elementary engineering fracture mechanics*. Springer.

Dowling, N. (2007). *Mechanical behavior of materials*. Pearson.

Fanani, E.W.A., Surojo, E., Prabowo, A. R., & Akbar, H. I. (2021). Recent progress in hybrid aluminum composite: manufacturing and application. *Metals, 11*(12), 1919-1929.

Gandra, J., Miranda, R., Vilaça, P., Velhinho, A., & Teixeira, J.P. (2011). Functionally graded materials produced by friction stir processing. *Journal of Materials Processing Technology, 211*(11), *1659-1668.*

Kaul, A. B. (2014). Two-dimensional layered materials: Structure, properties, and prospects for device applications. *Journals of Materials Research*, *29*, 348-361.

Mahamood, R. C., & Akinlabi, E. T. (2017). *Functionally graded materials*. Springer.

Obodovski, B. A., & Hanin, S. E. (1981). *Strength of materials*. Vista.

Radhika, N., Sasikumar, J., Sylesh, J. L., & Kishore, R. (2020). Dry reciprocating wear and frictional behaviour of B4C reinforced functionally graded and homogenous aluminium matrix composites. *Journal of Materials Research and Technology*, *9,* 1578-1592.

Rizov, V. I. (2018). Non-linear delamination in two-dimensional functionally graded multilayered beam. *International Journal of Structural Integrity, 9,* 646-663.

Rizov, V. I. (2024). Analysis of delaminated multilayered rod under centric impact. *AIP Conference Proceedings, 3078*, 060007.

Rizov, V.I. (2019). Influence of material inhomogeneity and non-linear mechanical behaviour of the material on delamination in multilayered beams. *Frattura ed Integrità Strutturale, 13*(47), 468-481.

Toudehdehghan, J., Lim, W., Foo1, K. E., Ma'arof, & M. I. N., Mathews J. (2017). A brief review of functionally graded materials. *MATEC Web of Conferences, 131,* 03010.

Udupa, G., Rao, S. S., & Gangadharan, K. V. (2014). Functionally graded composite materials: an overview. *Procedia Materials Science*, *5*, 1291-1299.

Author Information

Victor Rizov
Department of Technical Mechanics
University of Architecture, Civil Engineering and Geodesy
1 Chr. Smirnensky blvd. 1046 – Sofia, Bulgaria
Contact e-mail: *v_rizov_fhe@uacg.bg*

To cite this article:

Rizov, V. (2025). Influence of different behavior in tension and compression on longitudinal fracture of inhomogeneous beams under impact. *The Eurasia Proceedings of Science, Technology, Engineering and Mathematics (EPSTEM), 33,* 130-139.